Nuclear Instruments and Methods in Physics Research A 787 (2015) 78–84

Contents lists available at ScienceDirect

Nuclear Instruments and Methods in Physics Research A

journal homepage: www.elsevier.com/locate/nima

Pilot production & commercialization of LAPPD™

Michael J. Minot [a,*], Daniel C. Bennis [a], Justin L. Bond [a], Christopher A. Craven [a], Aileen O'Mahony [a], Joseph M. Renaud [a], Michael E. Stochaj [a], Jeffrey W. Elam [b], Anil U. Mane [b], Marcellinus W. Demarteau [b], Robert G. Wagner [b], Jason B. McPhate [c], Oswald Helmut Siegmund [c], Andrey Elagin [d], Henry J. Frisch [d], Richard Northrop [d], Matthew J. Wetstein [d]

[a] Incom Inc, 294 Southbridge Road, Charlton, MA 01507, USA
[b] Argonne National Laboratory, 9700 S. Cass Avenue, Lemont, IL 60439-4814, USA
[c] Space Sciences Laboratory, University of California, Berkeley, CA 94720, USA
[d] University of Chicago, 5640 S. Ellis Ave., Chicago, IL 60637, USA

ARTICLE INFO

Available online 25 November 2014

Keywords:
Large-area picosecond photodetectors (LAPPD)
Time of flight detector
Glass capillary array (GCA)
Microchannel plate (MCP)
Atomic layer deposition (ALD)

ABSTRACT

We present a progress update on plans to establish pilot production and commercialization of Large Area (400 cm^2) Picosecond Photodetector (LAPPD™). Steps being taken to commercialize this MCP and LAPPD™ technology and begin tile pilot production are presented including (1) the manufacture of 203 mm × 203 mm borosilicate glass capillary arrays (GCAs), (2) optimization of MCP performance and creation of an ALD coating facility to manufacture MCPs and (3) design, construction and commissioning of UHV tile integration and sealing facility to produce LAPPDs. Taken together these plans provide a "pathway toward commercialization".

1. LAPPD

The Large Area Picosecond Photodetector (LAPPD™) is a microchannel plate (MCP) based photodetector, capable of imaging, and having both high spatial and temporal resolution in a vacuum package with an active area of 400 cm^2. LAPPD™ are characterized by a uniquely simple design based upon an all-glass vacuum package comprised of top and bottom plates and square sidewall, each made of borosilicate float glass, depicted in Fig. 1.

Key design features of the LAPPD include: (a) an internal chevron pair stack of "next generation" MCPs produced by applying resistive and emissive coatings to borosilicate glass capillary array (GCA) substrates; (b) a modular all-glass detector package with conductive RF microstrips passing through a glass frit seal that hermetically bonds the side walls to the bottom anode plate while allowing electrical contact to the interior of the device; eliminating the need for metal electrical pins penetrating the evacuated detector package; (c) resistively coated spacers that function as high voltage (HV) dividers to distribute voltage across the MCP chevron stack, eliminating the need for separate electrical leads contacting the tops and bottoms of both MCPs; and (d) RF stripline anodes applied to the bottom plate with an analog bandwidth above 1.5 GHz for good spatial and temporal resolution [1].

1.1. MCP based photodetectors

MCP's consists of millions of conductive glass capillaries (4–25 μm in diameter) fused together and sliced into a thin plate [2]. Each capillary or channel works as an independent secondary-electron multiplier. Single electrons that hit a pore on one side of the plate convert into large bunches of electrons that cascade from the other side [3], with typical amplification from a pair of plates of 10^7. Fig. 2 (left) shows a large area glass capillary array (GCA) consisting of millions of 20 μm diameter pores with an overall size of 203 mm × 203 mm × 1.2 mm with an aspect ratio = 60:1, bias angle of 8°, and open area ratio of 60%. Atomic Layer Deposition (ALD) techniques are used to apply resistive and emissive coatings, converting the GCA into a high performance MCP. A high voltage is applied across the top and bottom surfaces of the MCP; a photocathode applied to the inside surface of the entrance window emits photo-electrons which are then accelerated to the microchannel plate structure for fast multiplication of signals, as depicted in Fig. 2 (right) [4].

MCP-based photodetectors offer many advantages over other sensors. They are compact, lightweight, have unmatched temporal and good spatial detection properties, and can provide two-dimensional imaging with correlated timing at the picosecond level. Despite rapid

* Corresponding author. Tel.: +1 508 909 2369; fax: +1 508 765 0041.
E-mail address: mjm@incomusa.com (M.J. Minot).

http://dx.doi.org/10.1016/j.nima.2014.11.025
0168-9002/

progress on various solid state detectors, vacuum based photon detectors still play a significant role in many high energy experiments where high speed detection of weak photon signals is critical. One of the biggest advantages of the vacuum devices over solid state ones is their fast response. The photo-electron conversion, or QE, is typically only fair (about 20–35%), but the devices are unmatched for high gain, low noise, and response time and (for MCP-based devices) space resolutions.

2. "Next generation" MCPs

An enabling component of the LAPPD™ is a chevron pair of large area (203 mm × 203 mm) "next generation" MCPs. The manufacture of these "next generation" large-area high performance MCPs has been facilitated by the convergence of two technological breakthroughs.

The first breakthrough is the ability to produce large blocks of hollow, micron-sized glass capillary arrays (GCAs) developed by Incom Inc. The Incom process is based on the use of hollow capillaries in the glass drawing process, eliminating the need to later remove core material by chemical etching. These substrate arrays are made using the following steps: (a) a single glass tube is heated and drawn under tension to form a hollow capillary; (b) multiple glass capillaries are assembled to form an assembly that is heated and drawn to form a multi-capillary bundle; (c) multi-capillary bundles are further assembled and heated under pressure to form a large fused block; (d) the fused capillary block is sliced as shown in Fig. 3, and finished into glass capillary array (GCA) wafers having the desired dimensions.

One benefit of this approach is that GCAs can be made without regard to the conventional limits of capillary length/diameter (L/d) ratios. Moreover, borosilicate glass (Pyrex® or similar) is considerably less expensive than the leaded glass required for prior-art techniques, eliminates the need for further chemical processing, has a low alkali content for reduced background noise, and is more environmentally friendly due to the absence of lead.

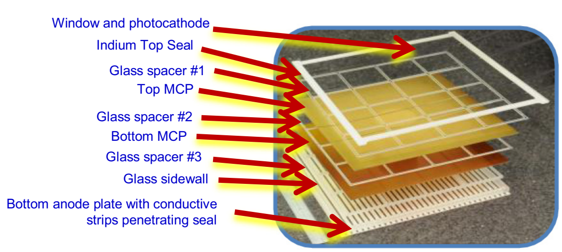

Fig. 1. LAPPD design features.

2.1. ALD coated MCPs

The second breakthrough enabling next generation MCPs was the advent of atomic layer deposition (ALD) coating methods and materials to coat or functionalize GCAs to impart the necessary resistive and secondary emission properties, converting them into highly effective MCPs with electronic gain and robust performance properties suitable for large area time of flight detector applications. ALD is a self-limiting, thin film deposition technique that sequentially applies alternating layers of reactant precursor chemicals to a surface to form a fully dense, conformal thin film. The volatile precursor reactants are introduced into the reaction chamber under reduced pressure. A key advantage of ALD is its ability to coat small pores with high L/d ratios. Nanocomposite ALD resistive coatings have been developed that meet all of the requirements for large area MCPs [5,6].

Large area MCPs must exhibit uniform performance over the full area of the device, and must be stable over time, irrespective of thermal history, or operation under high voltage, and high electron flux. ALD reactor design affects the flow dynamics and purging of precursor chemicals and has a direct effect on the uniformity of the resistive and emissive coatings. Subtle differences in the chemistry of multi-laminate ALD coatings, including interactions between the coatings and the glass substrate and can have a direct effect on the performance of the MCPs.

Equipment and process modifications were made to a commercial Beneq and custom-built ALD system to achieve coating uniformity and performance stability over large area MCPs. Fig. 4 (left) shows the Beneq TFS 500 used in these studies, as well as a fully functionalized 203 mm × 203 mm MCP produced using these techniques.

An important advantage of the ALD process for fabricating MCPs is the ability to separately apply and independently optimize the resistive and emissive layers, selecting from a wide variety of material options. This is not the case for conventional MCPs where a single lead sub-oxide resistive and emissive layer of variable composition is developed during a hydrogen reduction forming process.

3. Large area MCP performance results

The gain and spatial uniformity of functionalized MCP's are evaluated in a high vacuum system equipped with calibrated UV

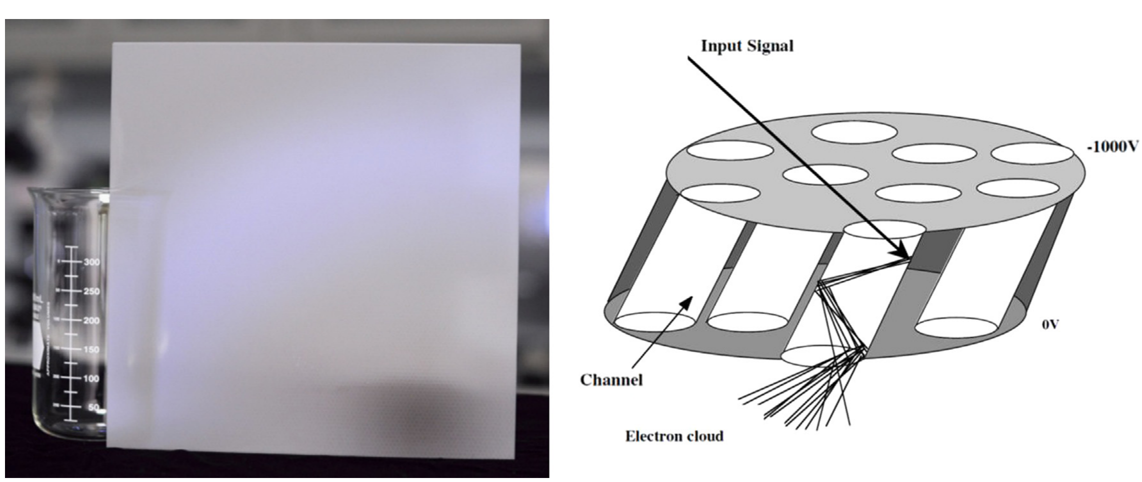

Fig. 2. (Left) Large-area, 203 mm square Incom GCA with 20 μm pores. (Right) Schematic of an MCP, showing the cascade of electrons generated from an incident electron.

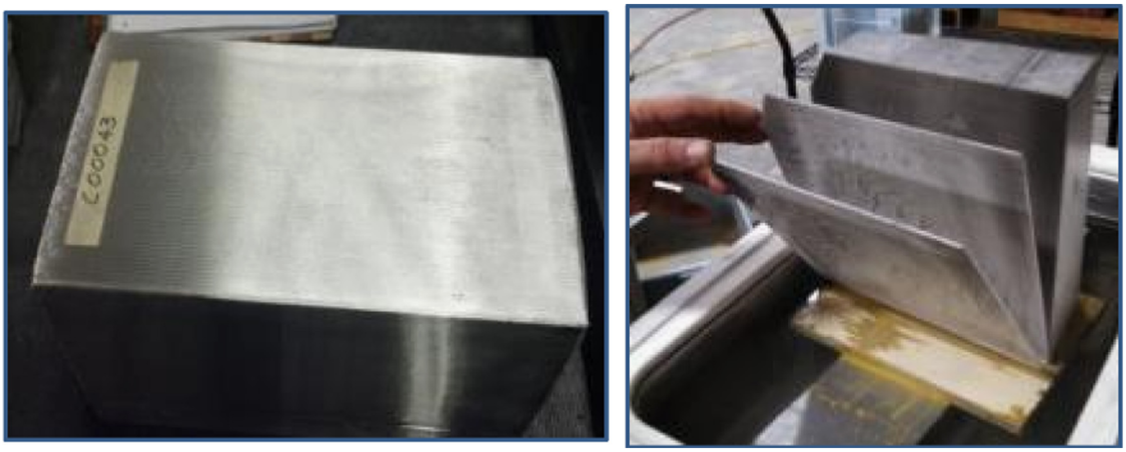

Fig. 3. (Left) Incom manufactures large blocks of hollow glass capillary arrays (GCAs) with micron-sized pores. (Right) Each block can be sliced to produce approximately 140–150 GCA 203 mm × 203 mm wafers that are later coated to produce high performance MCPs.

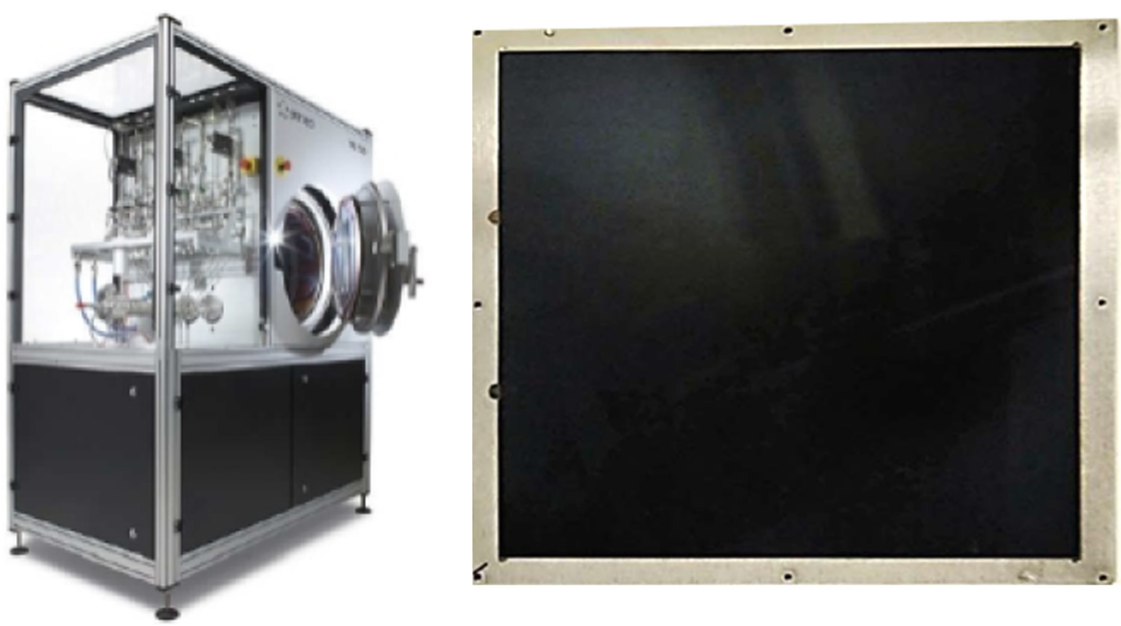

Fig. 4. (Left) Beneq ALD Coater, (right) fully coated MCP with resistive and emissive coatings, framed by a measurement and test fixture.

and electron sources and a photon counting /imaging readout anode. Fig. 5 shows the "as deposited" gain curve for a 203 mm × 203 mm MCP (#C00043-004), consisting of a borosilicate glass substrate ALD deposited with a resistive layer and MgO secondary electron emissive (SEE) layer. The gain for fully processed "next generation MCPs" (Fig. 7) is typically higher than achieved with commercial lead glass MCPs.

3.1. Attributes of the MgO secondary electron emissive (SEE) layer

The secondary electron yield (SEY) for conventional lead sub-oxide layers is ~2 (two secondary electrons produced for each primary electron striking the lead sub-oxide surface). The SEY of ALD applied Al_2O_3 and MgO exhibit SEYs of 3 and 7 respectively, and are dependent on the ALD coating thickness as shown [7] in Fig. 6. In addition to the higher secondary electron yield exhibited by MgO compared to Al_2O_3, the gain achieved with MgO increases during high current extraction "burn in".

The temporal stability of the MCP gain was examined by monitoring the gain versus time under a uniform illumination. The gain–voltage curves for "next generation" MCPs with an MgO SEE layer was found to be stable after several weeks of operation (Fig. 7 right) [8], and 1000 h of Nitrogen exposure. There is little outgassing during high temperature bake-out (350C), and for MCPs with an MgO SEE layer, the gain increases 10 fold during this bake-out (Fig. 7 left). In contrast, conventional MCPs exhibit a sharp initial decrease followed by a slow, gradual decay to a steady value. As a consequence of this behavior, conventional MCPs require a costly, time-consuming "scrubbing" treatment before they can be put into service. In contrast, ALD-coated borosilicate glass MCPs require significantly reduced scrubbing. After testing, storage under nitrogen, and retesting, the gain remained the same without the need for an initial or repeat burn-in (Fig. 7, left).

Fig. 8 is an MCP gain map taken using a cross delay line photon counting anode. Excitation of the MCP under test is achieved with 185 nm non-uniform UV illumination. Image striping is due to the anode period/charge cloud size modulation. The gain variability

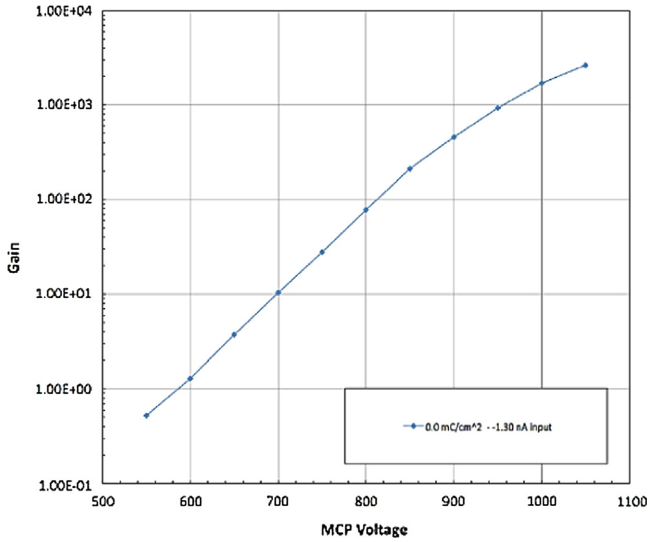

Fig. 5. "As deposited" gain curve for 203 mm × 203 mm MCP (#C00043-004), borosilicate glass substrate with ALD deposited Chem-1 resistive and MgO SEE layer.

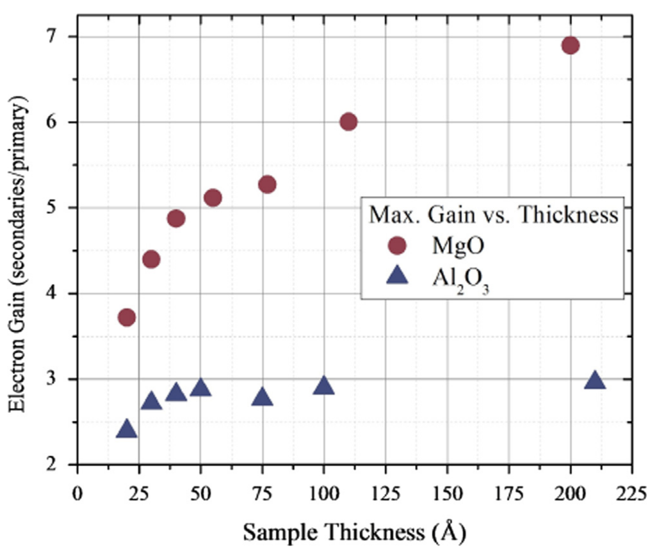

Fig. 6. MgO and Al_2O_3 have high secondary electron yields (7 and 3 respectively) which vary depending on thickness. By comparison, the SEY for conventional lead oxide glass based MCPs is ~2.

for this sample, over the 203 mm × 203 mm area of the MCP is < 15%. This compares favorably with that achieved with much smaller sized conventional MCPs currently available commercially.

The background for MCPs with borosilicate glass substrate is typically 0.055 counts s^{-1} cm^{-2}, over 2000 s, for $2k \times 2k$ imaging or about ~5 times lower than standard (PbO) glass MCPs. This lower background is attributed to the fact that the borosilicate glass substrates have considerably less Potassium-40 compared to the (PbO) glasses used for standard MCPs.

4. Fabrication of fully integrated sealed detector tiles

Integration of key device components including MCPs, photocathode, spacers, getters, and the anode stripline detector, to form a fully sealed detector tile, is presently done in collaboration with the Experimental Astrophysics Group, Space Sciences Laboratory (SSL), at University of California at Berkeley.

The bialkali photocathode used in these detectors is extremely sensitive to chemical and thermal exposure. As a consequence, the deposition of the photocathode must be done under ultra-high vacuum (UHV) in a tank that has been rigorously cleaned, baked-out and evacuated. Furthermore, once the photocathode is fabricated, it cannot tolerate high temperatures. The final seal joining the top window with photocathode applied, to the body tray containing the MCPs, spacers and anode, is made with a low temperature melting point alloy.

Device integration and sealing follows a multi-step procedure that has been developed and reliably demonstrated over time at SSL for smaller ceramic packages. Comparable processing applies to the "all glass" package, including cleanliness and out-gassing procedures of all components to eliminate virtual leaks, and to prepare surfaces for deposition of well adhered, sensitive films as well as wetting with metal alloys. The integration and sealing process includes: (a) preparation of detector tube internal parts, (b) detector internal stack assembly, and (c) bialkali photocathode deposition and d) device sealing.

The first (ceramic) 203 mm × 203 mm LAPPD tile integration and sealing trial was initiated in July, 2013. Fig. 9 (right) shows QE vs. wavelength for the photocathode deposited by co-evaporation of bialkali components during fabrication of tube #1. Successful deposition of several bialkali photocathodes with 20–25% QE at 350–400 nm and exhibiting ±15% uniformity over the 203 mm × 203 mm area plate was demonstrated. The QE improves as the photocathode cools. Similar photocathodes remained stable for over 5 months. Fig. 9 (left) plots the normalized QE at each location on the window and shows that QE was uniform within ±15%, except where obscured by tooling during deposition.

Once assembled and "sealed" the fully integrated tile was measured and characterized while still under vacuum in the UHV tank. Good gain uniformity was observed over the detector with a few localized "hot spots". Further testing was done with a 610 nm laser with a spot image of < 5 mm FWHM at high pulse amplitudes, show time resolution of 64 ps.

Unfortunately Tile #1 leaked when brought up to atmosphere due to an incomplete alloy seal of the top window. This tile, with readout electronics [9] is shown in Fig. 10 (left).

Several sealed tube detectors have now been built using "next generation" borosilicate MCPs coated by ALD. Fig. 10 shows a fully integrated sealed ceramic LAPPD, with Incom 203 mm × 203 mm MCP and readout electronics, as well as an image intensifier tube [10] incorporating an 86.6 mm diameter, 10 μ diameter pore × 0.46 mm thick "next generation" MCP. In addition, SSL has fabricated a 25 mm cross delay line readout sealed tube with an opaque GaN photocathode deposited on "next generation" MCPs, and has evaluated a commercial Photonis Planacon tube using a pair of ALD borosilicate MCPs.

The results achieved with Tile #1, have been augmented with test data from a fully integrated and working all glass "demountable" detector system. This demountable detector is an O-ring sealed, dynamically pumped detector tile test system [11] incorporating all of the design features of the LAPPD, substituting an Aluminum metal photocathode for bialkali. Table 1 summarizes actual demonstrated results that have been achieved with LAPPD detectors as well as the projected target performance expected for prototype LAPPD Tiles being commercialized.

5. LAPPD commercialization

The high energy physics (HEP), scientific and medical communities have expressed interest in exploiting the availability of high sensitivity photo-sensors with improved spatial and temporal

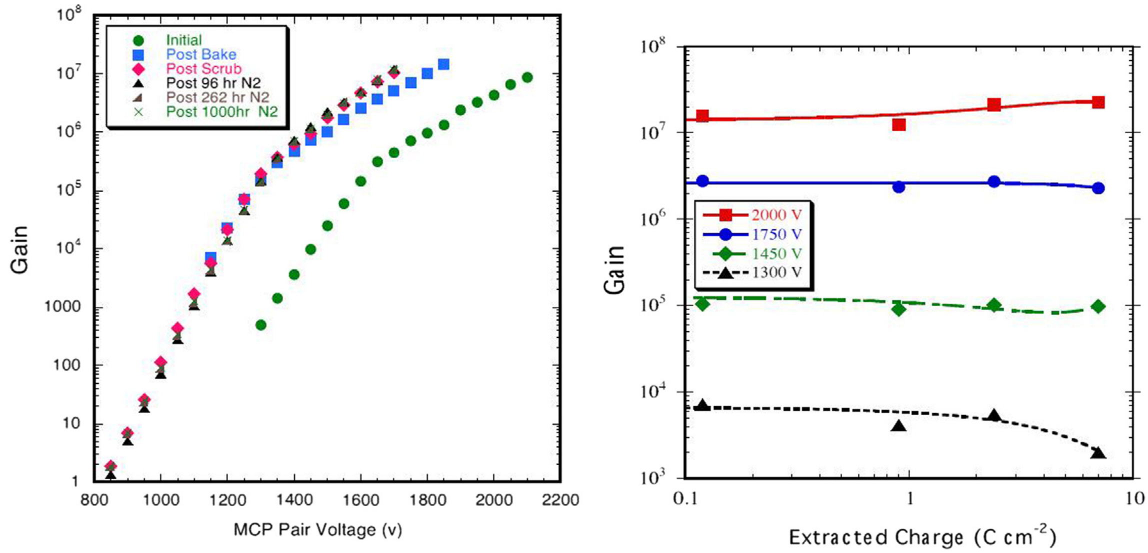

Fig. 7. (Left) Gain curves of MCP pair (20 μm pore, 60:1 *L*/*d*, 8° bias) at stages during preconditioning and nitrogen exposure. Right – UV scrub of ALD MCP pair 164–163, (20 μm pore, 60:1 *L*/*d*, 8° bias).

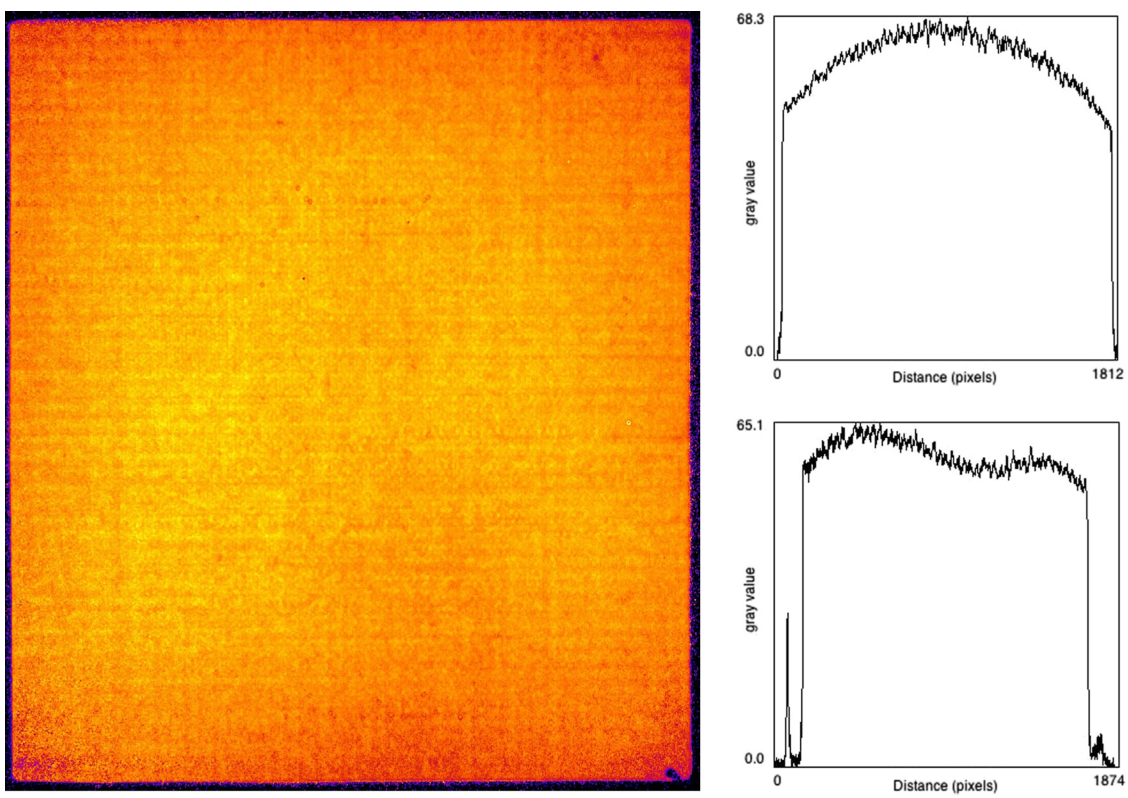

Fig. 8. (Left) Average gain image "map" across the 8" × 8" MCP (#C00043-004) made from borosilicate 20-μm pore GCA substrate, 60:1 *L*/*d* ratio and ALD deposited Chem-1 resistive coating, and MgO SEE layer. (Right) Gain uniformity along the *X*-axis and *Y*-axis. Showing < 15% overall variation.

resolution that can be scaled to large areas, and manufactured in a robust, durable and compact package at a low cost. The availability of large-area photodetectors with time resolutions below 10 ps and space resolutions of < 50 μm produced economically will enable new techniques in HEP for multiple vertex separation and particle identification at high-luminosity colliders, possible light collection in heavy-noble-liquid ionization detectors, high-resolution electromagnetic calorimeters, large non-cryogenic tracking neutrino detectors, and combinatorial photon background rejection in rare kaon-decay experiments. Other commercial applications of these devices will include detectors for mass spectrometers, medical imaging (PET), as well as neutron detection for scientific and homeland security (non-proliferation) applications.

A recently held "Early Adopters Users" meeting [12] attracted over 24 technical leaders and Principal Investigators, representing 17 High Energy Physics programs, demonstrating strong interest in LAPPD™ for beta testing. "Early Adopters" divided into multiple groups with different, but overlapping requirements depending on the specific mission of their program. Some applications will require high magnetic and radiation tolerance. Performance of LAPPD in high magnetic and radiation fields remains to be demonstrated, and will be evaluated by end users once prototype devices become

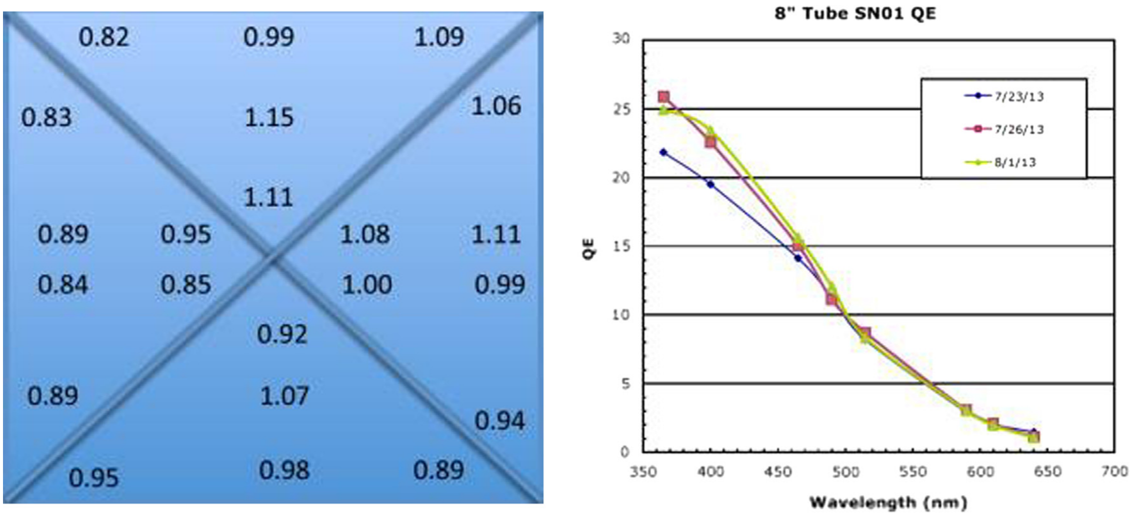

Fig. 9. (Right) QE vs. wavelength for photocathode deposited by co-evaporation of bialkali components during fabrication of tube #1. The QE improves as the photocathode cools. Similar photocathodes remained stable for over 5 months. (Left) Normalized QE was uniform within $\pm$15%, except where obscured by tooling during deposition.

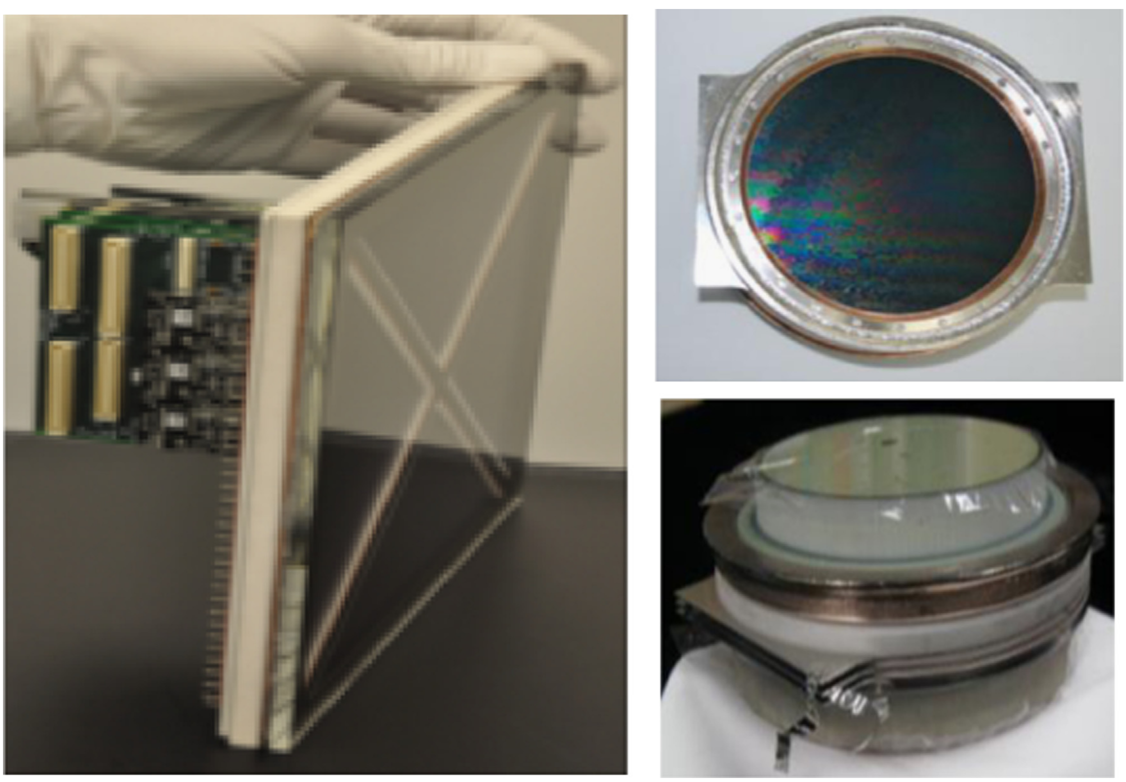

Fig. 10. (Left) Fully integrated sealed ceramic LAPPD, with Incom 203 mm $\times$ 203 mm MCP & readout electronics (Gary Varner, University of Hawaii). (Right top and bottom) Image intensifier tube: 86.6 mm diameter, 10 μ diameter pore $\times$ 0.46 mm thick Incom MCP.

Table 1
Demonstrated results and target performance for LAPPD tiles.

Parameter	Demonstrated results "Standard" LAPPD 20 μm *Φ* pores & future targets
MCP	Functional area 200 mm $\times$ 200 mm $\times$ 1.2 mm, 20 μm pore, pitch=25 μ, OAR=65%, flat $\pm$ 12.7 μm, resistive layer: 10–25 MΩ, optional SEE layer: MgO or Al_2O_3
MCP gain	10^5 @ 1400 V, 10^7 @ 2000 V, chevron pair
MCP gain uniformity	$<$15% edge to edge variability
MCP background rates	3000 s background, 0.085 events cm^{-2} s^{-1} at 7×10^6 gain, 1025v bias on each MCP. MCP background rate is about 35 kHz at the highest running gain.
QE	20–25% QE @350–400 nm, $\pm$15% uniformity over 200 mm $\times$ 200 mm area
Spatial resolution	1 mm for large signals, 5 mm for single photons (application specific) (with PSEC4 or PSEC5 read-out electronics and software algorithms)
Timing resolution	64 ps demonstrated single-photon, scales as $1/N$; single-photon target= $\le$40 ps(610 nm laser, spot image of $<$5 mm, FWHM at high pulse amplitudes)

available. There was general agreement however, that LAPPD design features should translate into a lower cost product compared to other MCP based photodetectors currently available. Furthermore, with continued development, the underlying technology appears to be amenable to still higher performance. Future pricing will depend on demonstrating an effective, high yield manufacturing process, with sufficient volumes to take advantage of economies of scale. Despite these uncertainties, it is already clear that the identified need translates into meaningful market demand.

The design, construction and commissioning of facilities necessary for pilot production of LAPPD is now underway at Incom Inc. These include expanded facilities to fabricate GCA's, functionalize them with ALD coatings to produce MCPs, and UHV tile integration and sealing facility for LAPPDs. Detector tile integration and sealing trials are planned with a target of demonstrating fully integrated sealed LAPPD detectors in fall 2014. General availability of prototype LAPPDs will be determined by the progress of the commercialization program described here but plans call for demonstrating pilot production of LAPPDs in 2015 and the delivery of initial LAPPD tiles to early adopters in 2016.

Acknowledgment

The authors would like to thank the U.S. Department of Energy for their continued financial support [13] Funding and the cooperation of the many institutions (Argonne National Laboratory, University of California at Berkeley, University of Chicago, University of Hawaii and Fermilab) that that have contributed to this work.

References

[1] H. Grabas, R. Obaid, E. Oberla, H. Frisch, J.-F. Genat, R. Northrop, F. Tang, D. McGinnis, B. Adams, M. Wetstein, Nuclear Instruments and Methods A71 (2013) 124.

[2] This concise MCP definition is credited to Hamamatsu.

[3] Argonne News: Robert Wagner, Award-winning technology provides a breakthrough in particle physics, by Jared Sagoff, ⟨http://www.anl.gov/articles/award-winning-technology-provides-breakthrough-particle-physics⟩, August 3, 2012.

[4] O.H.W. Siegmund, Methods of Vacuum Ultraviolet Physics, Chapter III, 2nd Edition, in: J.A.R Sampson, D.L. Ederer (Eds.), Academic Press, 1998.

[5] J.W. Elam, A.U. Mane, J.A. Libera, J.N. Hryn, O.H.W. Siegmund, J. McPhate, M.J. Wetstein, A. Elagin, M.J. Minot, A. O'Mahony, R.G. Wagner, H.J. Frisch, W.M. Tong, A.D. Brodie, ECS Transactions 58 (10) (2013) 249. http://dx.doi.org/10.1149/05810.0249ecst.

[6] A.U. Mane, J.W. Elam, Chemical Vapor Deposition 19 (2013) 186. http://dx.doi.org/10.1002/cvde.201307054.

[7] Slade J. Jokela, Igor V. Veryovkin, Alexander V. Zinovev, Jeffrey W. Elam, Anil U. Mane, Qing Peng, Zinetulla Insepov, Physics Procedia 37 (2012) 740.

[8] O.H.W. Siegmund, J.B. McPhate, A.S. Tremsin, J.V. Vallerga, C.D. Ertley, N.J. Richner, T.M. Gerard, H.J. Frisch, J.W. Elam, A.U. Mane, R.G. Wagner Application of Atomic Layer Deposited Microchannel Plates to Imaging Photodetectors with High Time Resolution, Presented NDIP, 2014.

[9] PSEC4 or PSEC5 Read-out Electronics were Developed and Supplied by Gary Varner University of Hawaii.

[10] E. Dutra, D. Max, J. O'Connor, R. Buckles, Integrated Micro-Channel Plate Collaboration with Incom, National Securities Technologies, LLC, DOE/NV/25946-2251, Confidential communication, 2014.

[11] B. Adams, M. Chollet, A. Elagin, A. Vostrikov, M. Wetstein, R. Obaid, P. Webster, Laser Review of Scientific Instruments 84 (2013) 061301.

[12] Early Adopters Meeting, held at Incom Inc., Charlton, MA, November 18, 2013.

[13] Funding from the United States Department of Energy – Grant # DE-SC0009717, TTO Ph II, "Fully Integrated Sealed Detector Devices," 4/15/14–4/14/16.